

Large-scale heterochromatin remodeling linked to overreplication-associated DNA damage

Wei Feng^{a,1}, Christopher J. Hale^b, Ryan S. Over^a, Shawn J. Cokus^b, Steven E. Jacobsen^{b,c,2}, and Scott D. Michaels^{a,2}

^aDepartment of Biology, Indiana University, Bloomington, IN 47405; ^bDepartment of Molecular, Cell and Developmental Biology, University of California, Los Angeles, CA 90095; and ^cHoward Hughes Medical Institute, University of California, Los Angeles, CA 90095

Contributed by Steven E. Jacobsen, December 2, 2016 (sent for review April 8, 2016; reviewed by Ortrun Mittelsten Scheid and Nathan M. Springer)

Previously, we have shown that loss of the histone 3 lysine 27 (H3K27) monomethyltransferases ARABIDOPSIS TRITHORAX-RELATED 5 (ATXR5) and ATXR6 (ATXR6) results in the overreplication of heterochromatin. Here we show that the overreplication results in DNA damage and extensive chromocenter remodeling into unique structures we have named “overreplication-associated centers” (RACs). RACs have a highly ordered structure with an outer layer of condensed heterochromatin, an inner layer enriched in the histone variant H2AX, and a low-density core containing foci of phosphorylated H2AX (a marker of double-strand breaks) and the DNA-repair enzyme RAD51. *atxr5,6* mutants are strongly affected by mutations in DNA repair, such as ATM and ATR. Because of its dense packaging and repetitive DNA sequence, heterochromatin is a challenging environment in which to repair DNA damage. Previous work in animals has shown that heterochromatic breaks are translocated out of the heterochromatic domain for repair. Our results show that *atxr5,6* mutants use a variation on this strategy for repairing heterochromatic DNA damage. Rather than being moved to adjacent euchromatic regions, as in animals, heterochromatin undergoes large-scale remodeling to create a compartment with low chromatin density.

ATXR5 | ATXR6 | H3K27me1 | DNA repair | DNA replication

Posttranslational modifications of histones play key roles in nearly all aspects of chromatin biology. The methylation of histone 3 lysine 27 (H3K27) is a well-characterized modification with critical functions in the repression of gene expression (1, 2). In particular, H3K27 trimethylation (H3K27me3), which is catalyzed by the Polycomb repressor complex 2 (PRC2), is essential for the control of developmentally regulated genes. The SET domain-containing enhancer of zeste [E(z)] homologs act as the catalytic subunits of PRC2 complexes. In animals, E(z) proteins are responsible for all levels of H3K27 methylation (i.e., H3K27me1, H3K27me2, and H3K27me3). Plants, in contrast, have divided H3K27 methylation activity between two groups of SET-domain proteins (3). *Arabidopsis* contains three E(z) homologs: MEDEA, CURLY LEAF, and SWINGER. Plants with mutations in these genes or in other PRC2 components show strong reductions in H3K27me2 and H3K27me3 (4–9). H3K27me1, however, was relatively unaffected (10), suggesting that this modification was catalyzed by another group of enzymes.

ARABIDOPSIS TRITHORAX-RELATED 5 (ATXR5) and ARABIDOPSIS TRITHORAX-RELATED 6 (ATXR6) act as H3.1-specific H3K27 monomethyltransferases (11–14). Unlike H3K27me3, which is typically associated with the regulated repression of genes, H3K27me1 is associated with the constitutive repression of transposons and DNA repeats. In *Arabidopsis*, these sequences are enriched in pericentromeric regions and are compacted into DAPI-dense regions called “chromocenters” (15), which are marked by repressive modifications such as H3K27me1, H3K9me2, and DNA methylation (10, 16–18). *atxr5,6* mutants show a strong reduction in H3K27me1, particularly in endoreduplicated (e.g., 8C and 16C) leaf cells. Although DNA methylation and H3K9me2 are largely unaffected in *atxr5,6* mutants, there is a partial loss of gene silencing (11). *atxr5,6* mutants also show an

overreplication of heterochromatic regions of the genome (11, 12). This overreplication may be triggered by the presence of unmethylated K27 on H3.1 in *atxr5,6* mutants. This model is supported by two observations indicating that removal of H3.1 can suppress overreplication. First, mutations in DNA methylation or H3K9me2, which lead to the large-scale loss of gene silencing and the replacement of H3.1 with H3.3, are able to suppress overreplication in *atxr5,6* mutants (13). Likewise, mutations that prevent the loading of H3.1 into chromatin also suppress overreplication (14).

Results and Discussion

In our previous characterization of *atxr5,6* double mutants, we noted the partial decondensation of chromocenters (11). Upon closer examination, however, we found that chromocenters in *atxr5,6* nuclei often had a unique hollow appearance, with a densely staining shell of heterochromatin surrounding a less DAPI-bright interior, that was not observed in wild-type nuclei (Fig. 1 A and B). We speculated that these remodeled chromocenters might result from a loss of gene silencing and/or the overreplication of heterochromatin, both of which occur in *atxr5,6* mutants. To determine if gene-silencing defects alone would lead to the creation of hollow chromocenters, we examined the nuclei of DNA methylation (*ddm1*) and H3K9me2 (*suvh4,5,6*) mutants (18, 19). These mutations lead to a more pronounced loss of gene silencing than the *atxr5,6* mutation but do not cause DNA

Significance

Heterochromatin is a challenging environment in which to repair DNA damage. In addition to dense packaging, heterochromatin often contains repetitive DNA that can lead to errors in homologous recombination-based repair. One strategy to address this problem has been reported in animals. In *Drosophila*, heterochromatic double-strand breaks are translocated out of the heterochromatin into nearby euchromatin for repair. Here, we show that ARABIDOPSIS TRITHORAX-RELATED 5,6 (*atxr5,6*) mutants use an interesting variation of the approach used by animals. Rather than translocating heterochromatic breaks into euchromatin, heterochromatic aggregations, called “chromocenters,” are remodeled to create specialized compartments with reduced chromatin density. These compartments contain double-strand breaks and DNA-repair enzymes and therefore are likely to play a role in facilitating heterochromatic DNA repair.

Author contributions: W.F. and S.D.M. designed research; W.F., C.J.H., and R.S.O. performed research; S.E.J. contributed new reagents/analytic tools; W.F., C.J.H., S.J.C., S.E.J., and S.D.M. analyzed data; and S.D.M. wrote the paper.

Reviewers: O.M.S., Gregor Mendel Institute of Molecular Plant Biology, Austrian Academy of Sciences; and N.M.S., University of Minnesota.

The authors declare no conflict of interest.

¹Present address: Department of Plant Biology, Carnegie Institution for Science, Stanford, CA 94305.

²To whom correspondence may be addressed. Email: michaels@indiana.edu or jacobsen@ucla.edu.

This article contains supporting information online at www.pnas.org/lookup/suppl/doi:10.1073/pnas.1619774114/-DCSupplemental.

regions [i.e., being more abundant in pericentromeric heterochromatin than in the arms of the chromosomes (12)], it should be noted that processes other than overreplication, such as replication-dependent DNA repair, could also account for or contribute to this pattern of EdU incorporation.

Overreplication is known to lead to genomic instability and DNA damage, including double-strand breaks (24–28). Consistent with this observation, many DNA damage-response genes, including BRCA1, PARP1, CYCB, and RAD51 (Fig. 2B), are up-regulated in *atr5,6* mutants (13), and evidence of breaks was detected in comet assays (Fig. S2). To determine if damaged DNA is associated with RACs, we performed immunolocalization with an antibody recognizing γ -H2AX, a phosphorylated form of the histone variant H2AX, which is associated with sites of double-strand breaks (29, 30). γ -H2AX was not detected in the wild-type nuclei (Fig. 2C); however, foci of γ -H2AX staining were visible following γ -irradiation (Fig. S3). Consistent with overreplication inducing double-strand breaks, γ -H2AX staining was observed in *atr5,6* nuclei and, fascinatingly, the γ -H2AX foci were localized to the centers of RACs (Fig. 2D). As with overreplication, the amount of γ -H2AX staining was highest in 8C and 16C nuclei (Fig. S4). Interestingly, γ -H2AX staining and EdU incorporation were rarely observed in the same nucleus (<1%), suggesting that overreplication and DNA damage recognition/repair are temporally separated. To determine if DNA damage might be sufficient to induce RAC formation in wild-type plants, we treated plants with γ -irradiation or hydroxyurea, a replication inhibitor. RACs were not observed in either case (Figs. S3 and S5), suggesting that the formation of RACs in *atr5,6* nuclei may require a higher density of DNA damage localized to chromocenters/pericentromeric heterochromatin than can be achieved with γ -irradiation or hydroxyurea. A non-mutually exclusive explanation may be that the reduction of H3K27me1 in *atr5,6* mutants plays a role in facilitating chromatin restructuring in chromocenters.

In addition to γ -H2AX, we examined the localization of total H2AX using a GFP::H2AX reporter construct driven by the 35S promoter (31). In wild-type plants, GFP::H2AX distribution appeared relatively uniform throughout the euchromatin (Fig. 2C); the observation that the chromocenters were not visible in the GFP::H2AX image suggests that H2AX is relatively less abundant in the constitutive heterochromatin (32). In *atr5,6* mutants, in contrast, GFP::H2AX was enriched in RACs (Fig. 2D). A similar pattern was observed when GFP::H2AX was driven with the endogenous H2AX promoter (Fig. S6). The shift in GFP::H2AX localization was confirmed by CHIP-sequencing (ChIP-seq). In wild-type plants, GFP::H2AX is less abundant in pericentromeric heterochromatin than in the euchromatic arms of the chromosomes, but GFP::H2AX is distributed more uniformly in *atr5,6* mutants (Fig. 2E). We did not detect specifically localized increases in GFP::H2AX at previously identified sites of overreplication (12), suggesting that the redistribution of GFP::H2AX may be associated with general remodeling of the chromocenter, rather than specifically marking sites of overreplication/DNA damage. Interestingly, the mechanism responsible for the relocation of H2AX observed in *atr5,6* mutants may be conserved in animals, because recent work in human cells has demonstrated a relocation of H2AX to genomic locations that are under replication stress (33).

Further immunolocalization analysis showed that RACs have a highly ordered, layered structure. The outermost layer consists of DAPI-bright H3K9me2-enriched heterochromatin followed by a layer containing GFP::H2AX (Figs. 2D and 3A). Previous ChIP-seq analysis has shown that the distribution of H3K9me2 is not changed in *atr5,6* mutants (11). Thus, the reorganization of H3K9me2 observed by immunolocalization is likely caused by the movement of chromatin rather than by the redistribution of H3K9me2 to other DNA sequences. Single-plane images of individual RACs revealed a core that is depleted in both H3K9me2

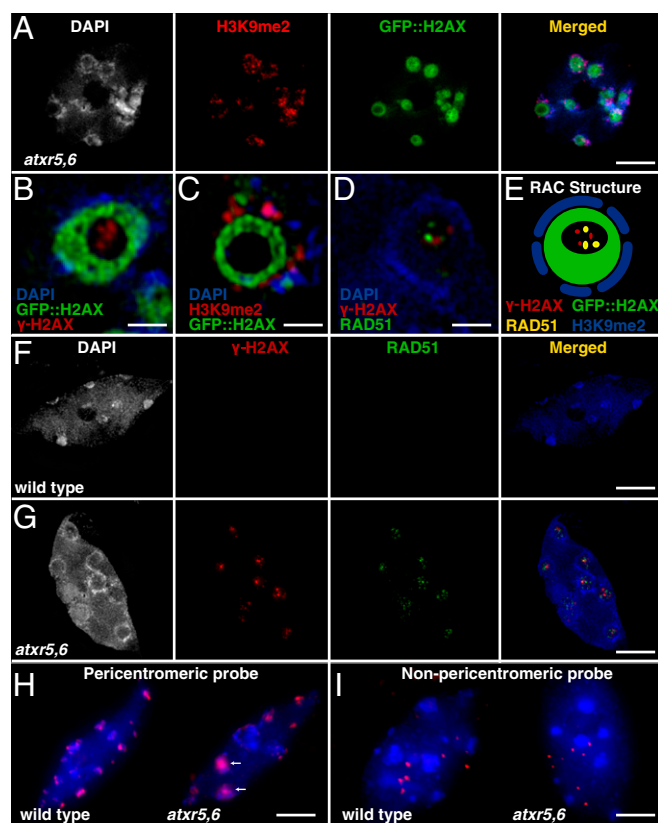


Fig. 3. RACs have a layered structure and contain γ -H2AX and RAD51 foci. (A) H3K9me2 and GFP::H2AX localize to distinct domains. (B–D) Single-plane images through individual RACs. (E) A schematic representation of RAC structure. (F and G) Immunolocalization of γ -H2AX and RAD51. (H and I) FISH analysis using probes containing pericentromeri (H) or non-pericentromeric (I) overreplicating regions. Arrows indicate hybridization inside RACs. Scale bars: 5 μ m in A, F, G, H, and I; 1 μ m in B–D.)

and GFP::H2AX (Fig. 3B and C). Distinct foci of γ -H2AX exist in the core, suggesting the presence of double-strand breaks. To determine if the core region of RACs might be associated with DNA repair, we examined the localization of the DNA-repair protein RAD51 (34). Like γ -H2AX, RAD51 is localized to distinct foci in RAC core regions (Fig. 3D–G). Thus, in response to *atr5,6*-induced overreplication, *Arabidopsis* chromocenters undergo a remarkable remodeling to form previously unidentified subnuclear structures that are associated with DNA repair.

In *atr5,6* mutants, the majority of overreplication occurs in pericentromeric heterochromatin/chromocenters (12). Thus, RACs are spatially associated with the bulk of overreplication-associated DNA damage. However, overreplication also occurs at a smaller number of sites outside the pericentromeric heterochromatin, i.e., at \sim 400 sites (often transposons) in the euchromatic chromosome arms (12). To determine if RACs also might play a role in the repair of damage at sites outside the pericentromeric heterochromatin, we used FISH to localize pericentromeric and non-pericentromeric sites known to overreplicate in the *atr5,6* mutant. As expected, a pericentromeric probe localizes to chromocenters in wild-type plants and can be observed inside RACs in *atr5,6* mutants (Fig. 3H). Non-pericentromeric overreplication regions, however, are not associated with pericentromeric heterochromatin in wild-type plants or *atr5,6* mutants (Fig. 3I). This localization suggests that RACs function primarily in the repair of local DNA damage originating from overreplication events in the pericentromeric heterochromatin.

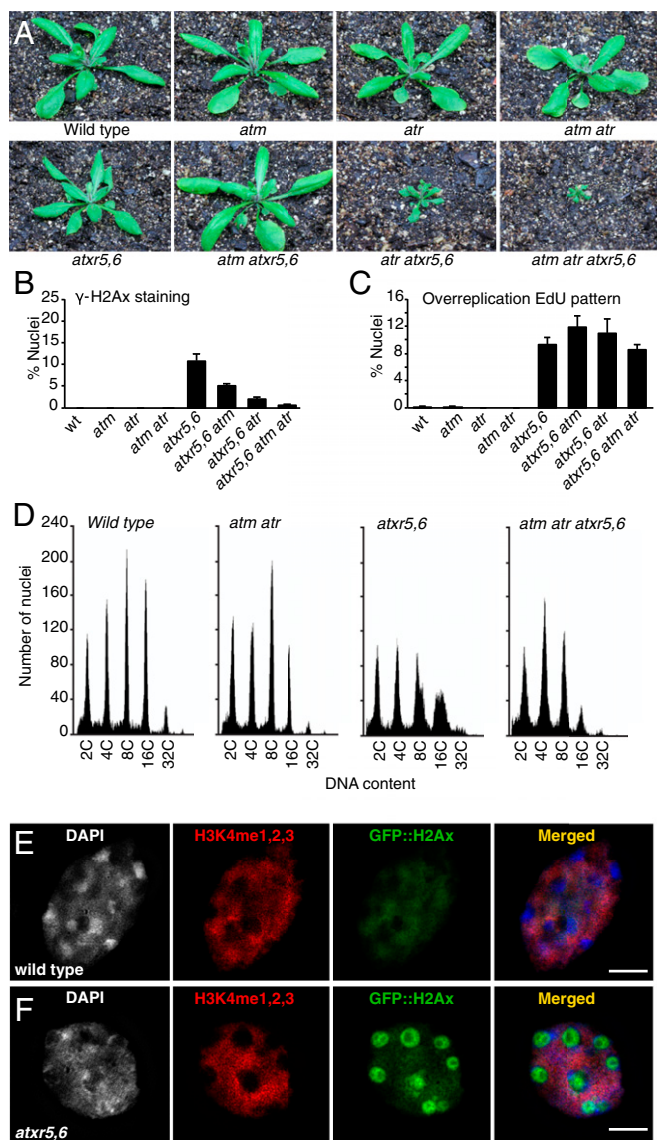


Fig. 4. *atxr5,6* mutants are strongly affected by defects in DNA repair. (A) *atm*, *atr*, and *atm atr* double mutants in wild-type and *atxr5,6* backgrounds. (B and C) Percentage of nuclei with chromocenter γ -H2AX staining (B) and an overreplication pattern of EdU incorporation (C). Error bars represent 1 SD. (D) Determination of DNA content by flow cytometry. Five thousand nuclei were analyzed for each genotype. (E and F) H3K4 methylation, a euchromatic mark, is not enriched in RACs. (Scale bars: 5 μ m.)

To investigate the relationship between overreplication and DNA damage further, we crossed *atxr5,6* plants with mutants that are defective in DNA-damage repair. ATM and ATR are two key protein kinases that mediate DNA-damage responses by triggering phosphorylation cascades. Targets of ATM/ATR include H2AX and other proteins involved in DNA repair. In *Arabidopsis*, *atm* and *atr* single mutants and *atm atr* double mutants appear similar to wild-type plants (Fig. 4A). Comparatively low levels of DNA damage in these otherwise wild-type plants may explain the relatively benign effects of loss of *ATM/ATR*. We speculated that elevated levels of DNA damage caused by overreplication would make *atxr5,6* mutants more dependent on *ATM/ATR*. This is indeed the case. *atxr5,6* and *atm atxr5,6* plants are relatively normal, but *atr atxr5,6* plants show reduced size and abnormal growth (Fig. 4A). These pleiotropic phenotypes are even more severe in the *atm atr atxr5,6* quadruple mutant. These

results indicate that both *ATM* and *ATR* are required for the repair of overreplication-associated DNA damage in *atxr5,6* mutants, with *ATR* playing the more major role. Consistent with the role of ATM/ATR in phosphorylating H2AX, γ -H2AX immunostaining was observed much less frequently in *atm atr atxr5,6* double mutants than in *atxr5,6* mutants (Fig. 4B). Interestingly, the number of nuclei showing increased DNA content was reduced in *atm atxr5,6*, *atr atxr5,6*, and *atm atr atxr5,6* mutants relative to *atxr5,6* mutants (Fig. 4D), suggesting that the loss of *atm/atr* might suppress rereplication. We found, however, that the number of nuclei showing overreplication EdU patterns in *atm atr atxr5,6* mutants was not significantly different from that in *atxr5,6* mutants (Fig. 4C). Thus, the reduction in nuclei with abnormally high DNA content in *atm/atr* mutants is not likely the result of reduced overreplication but may reflect reduced stability of overreplicated DNA (e.g., degradation) or decreased cell viability. The latter model is consistent with results in mammalian cells in which the knockdown of ATR in re-replicating cells has been shown to trigger apoptosis (28).

Given that many components of DNA repair are conserved, it is likely that plants and animals face similar challenges in the repair of heterochromatic DNA damage. Dense packaging and the presence of highly repetitive DNA sequences is thought to make heterochromatin a difficult environment in which to repair double-strand breaks (35). In *Drosophila*, radiation-induced heterochromatic breaks are translocated out of the heterochromatin for repair (36). In this process, RAD51 foci do not form until after the breaks have moved out of the heterochromatic domain (36). In *Arabidopsis*, rather than breaks being moved out of the heterochromatin and into/near euchromatin, as occurs in flies, heterochromatin is remodeled to create a less condensed compartment (i.e., RACs) for DNA repair. Although chromatin in the interior of RACs is significantly less dense than the surrounding heterochromatin, it is not enriched in modifications typical of euchromatin, such as histone 3, lysine 4 (H3K4) methylation (Fig. 4E and F). In summary, our work suggests that plants and animals have evolved fascinating variations on a similar theme for repairing heterochromatic DNA damage.

Methods

Plant Material and Growth Conditions. *atxr5,6* (11), *ddm1-3*, *kyp suvh5 suvh6*, *atxr5,6 ddm1-3*, *atxr5,6 kyp suvh5 suvh6* (13), and *atr-2* (37) mutants have been described previously. The transfer DNA (T-DNA) insertion mutant *atm-4* (SALK_040423C) was obtained from the *Arabidopsis* Biological Resource Center (ABRC). All plants were grown under cool-white fluorescent light (100 mol \cdot m $^{-2}$ \cdot s $^{-1}$) under long-day conditions (16 h of light followed by 8 h of darkness).

Genotyping. The following primers were used for genotyping:

ATM wild-type allele: *atm-4-F* (5'-CACAAAGCAGCAACGGTCAAGG) and *atm-4-R* (5'-AAGGGTTTCATCGGATATGCCGT); *atm-4* T-DNA allele: *atm-4-R* and Salk-LBa1 (5'-TGGTTCACGTAGTGGCCATCG).

Constructs. For 35S::GFP::H2AX, genomic H2AX (At1g08880, from start codon to stop codon) was amplified by PCR using the primers H2AX-CDS-F (5'-CACCATGAGTACAGGCGCAGGAAGCG) and H2AX-STOP-R (5'-TCAGAACTCCTGAGAAGCAGATCCAAT) and was cloned into *pENTR/D* (Invitrogen). To make the N-terminal GFP-tagged construct, the H2AX-*pENTR/D* insert was moved into pMDC43 (38) by Gateway LR cloning. *atxr5,6* plants were transformed by floral dip (39). *atxr5,6* plants homozygous for 35S::GFP-H2AX were crossed to wild-type plants to generate 35S::GFP-H2AX in Col. For pH2AX::GFP::H2AX, H2AX with its promoter (542 bp) was amplified from genomic DNA using the primers H2AX_p_F (CACCCTGTATTTCTGTTCTTAATAGTCTTCAC) and H2AX-CDS-R (GAACTCTGAGAAGCAGATCCAATATC) and was cloned into *pENTR/D* (Invitrogen) and moved into pMDC107 by Gateway LR cloning.

Antibodies. Antibodies used for ChIP and immunofluorescence assays were γ H2AX (613402; BioLegend), H3K9me2 (ab1220; Abcam), RAD51 (ab46981; Abcam), H3K4me1,2,3 (05-791; Millipore), and GFP (A-11122; Invitrogen).

Immunofluorescence and FISH. Immunofluorescence and FISH were performed as described previously (11). Probes used for FISH, F17A20 (pericentromeric) and F2J17 (non-pericentromeric), were obtained from the ABRC.

Imaging. Microscopy was performed in the Indiana University Light Microscopy Imaging Center using an Applied Precision DeltaVision personal DV Live Cell Imaging System and an OMX 3D-SIM Super-Resolution system. z-series images of individual nuclei were taken and processed (deconvolution and alignment) using Softworx imaging software. Representative z-stacked images are shown, unless stated otherwise.

ChIP and Sequencing. The ChIP protocol was adapted from ref. 40. Briefly, rosette leaves of 4-wk-old plants were collected, fixed in 25 mL MC buffer [10 mM sodium phosphate (pH 7), 50 mM NaCl, and 0.1 M sucrose] with 1% formaldehyde under vacuum for 30 min. Fixation was stopped by adding 2.5 mL of 1.25 M glycine. Fixed leaves were washed with MC buffer, dried on paper towels, and ground to a fine powder in liquid nitrogen. Two grams of powder were mixed with 30 mL M1 buffer [10 mM sodium phosphate (pH 7), 0.1 M NaCl, 10 mM β -mercaptoethanol, and complete protease inhibitor mixture] and were filtered through Miracloth (Millipore) into a 50-mL tube. Centrifugation was performed at $1,000 \times g$ for 20 min at 4 °C to pellet nuclei. The nuclear pellet was washed five times with 5 mL M2 buffer [10 mM sodium phosphate (pH 7), 0.1 M NaCl, 10 mM $MgCl_2$, 0.5% Triton X-100, 10 mM β -mercaptoethanol, and complete protease inhibitor mixture] and once with 5 mL of M3 buffer [10 mM sodium phosphate (pH 7), 0.1 M NaCl, and complete protease inhibitor mixture] by centrifuging at $1,000 \times g$ for 10 min at 4 °C. The nuclear pellet was resuspended in 1 mL of sonication buffer [10 mM sodium phosphate (pH 7), 0.1 M NaCl, 0.5% sodium lauryl sarcosinate and 10 mM EDTA] and was transferred to a 2-mL Eppendorf tube. Sonication of chromatin was performed with a water bath sonicator (Diagenode Bioruptor UCD-200) set on high with five 5-min rounds of 30-s on/30-s off with 1 min of cooling between each round. After centrifuging at $12,000 \times g$ for 15 min at 4 °C, the supernatant was transferred to a new 2-mL Eppendorf tube containing an equal volume of immunoprecipitation (IP) buffer [50 mM HEPES (pH 7.5), 150 mM NaCl, 5 mM $MgCl_2$, 10 μ M $ZnSO_4$, 1% Triton X-100, and 0.05% SDS] containing antibody or an equivalent amount of antiserum. Incubation was performed at 4 °C overnight with rotation. Fifty microliters of magnetic beads (Dynabeads Protein G, 100-03D; Invitrogen) were added to each sample, and incubation was resumed for another hour. The beads were recovered using a magnetic rack and were washed five times in IP buffer. Protein-DNA complexes were eluted from the beads by adding 100 μ L elution buffer (1% SDS and 0.1 M $NaHCO_3$) and were reverse-crosslinked by adding proteinase K (to final concentration of 0.5 mg/mL) and overnight incubation at 37 °C and 6 h incubation at 65 °C. DNA precipitation was performed with 2.5 vol 100% ethanol, 1/10 vol of 3 M NaAc (pH 5.4), and 1 μ L glycogen overnight at -20 °C. DNA was recovered by centrifugation at $12,000 \times g$ for 30 min at 4 °C and was resuspended in 100 μ L milliQ water.

ChIP-seq libraries were prepared using the Ovation Ultralow DR library construction kit (NuGen) as previously described (41). Sequence alignment and downstream data processing also were performed as previously described (41) with the exception that the *Arabidopsis* TAIR10 genome assembly was used in this study.

FACS Analysis. FACS analysis was performed as described previously (12).

Gene-Expression Analysis. Total RNA isolation and RT and real-time quantitative PCR analysis were performed as described previously (12). All experiments were replicated at least three times with similar results.

The following primers were used for qPCR:

BRCA1-qPCR-F, 5'-GCTGAAAAACCAAGGACTACACT
BRCA1-qPCR-R, 5'-GTTCTCCCATCATCTTCATCTCT
PARP1-qPCR-F, 5'-GCGTGAGGAAGCTATTAAGAGAGG
PARP1-qPCR-R, 5'-CTGTCCCATCTGATTTGACTG
CYCB1-qPCR-F, 5'-CTCAAGCATCACACTGGCTATTCT
CYCB1-qPCR-R, 5'-CGTTCGCTTGGAGTATTTCTT
RAD51-qPCR-F, 5'-CAACAACAAGACGATGAAGAAACC
RAD51-qPCR-R, 5'-GATCCTCTCGGAGTATAAGCAA
ACTIN2-qPCR-F, 5'-GCTGAGAGATTCAGATGCCCA
ACTIN2-qPCR-R, 5'-GTGGATTCCAGCAGCTTCCAT

EdU Assay. EdU assays were performed with the Click-iT EdU Imaging Kit (Invitrogen) according to the manufacturer's instructions (42). Briefly, *Arabidopsis* leaves were detached and sliced into small pieces and then were cultured in Murashige and Skoog media with 10 μ M EdU for 1 h. Then the samples were fixed in Tris buffer [10 mM Tris-HCl (pH 7.5), 10 mM NaEDTA, 100 mM NaCl] containing 4% formaldehyde. After two washings in Tris buffer, samples were transferred to 1.5-mL tubes, and 500 μ L Click-it reaction mix was added to each tube. The tubes were placed in darkness for 30 min at room temperature. After two washings in Tris buffer, nuclei were extracted by chopping the samples with a razor blade in LB01 buffer [15 mM Tris-HCl (pH 7.5), 2 mM NaEDTA, 0.5 mM spermine-4HCl, 80 mM KCl, 20 mM NaCl, and 0.1% Triton X-100]. The nuclei suspension was filtered through a 40- μ m cell strainer and mixed with two volumes of sorting buffer [100 mM Tris-HCl (pH 7.5), 50 mM KCl, 2 mM $MgCl_2$, 0.05% Tween-20, and 5% sucrose]. When immunolocalization was also performed, 12 μ L of the nuclei suspension was dried on the top of a coverslip followed by immunofluorescence procedures (11).

Comet Assay. Comet assays were performed by using the CometAssay kit (Trevigen) with minor modifications as described by Wang and Liu (43). To minimize photodamage, the protocol was carried out in dim light. Leaves from 4-wk-old plants were chopped with a razor blade in a Petri dish kept on ice and containing 500 μ L of $1 \times$ PBS plus 20 mM EDTA. After filtering through a 40- μ m strainer, 10 μ L of the nuclei suspension were mixed with 100 μ L of molten 1% low-melting-point agarose (kept at 37 °C) and was placed immediately onto two CometSlides. The slides were chilled at 4 °C for approximately 2 min and then were immersed in cold lysis solution [2.5 M NaCl, 100 mM EDTA (pH 10), 10 mM Tris, 1% sodium lauryl sarcosinate, and 1% Triton X-100] for 30 min at 4 °C. After washing in $1 \times$ Tris-borate/EDTA (TBE) for 15 min, the slides were run at 1 V/cm for 10 min in $1 \times$ TBE and were incubated in H_2O and 70% ethanol for 5 min each. After air-drying, the slides were stained with a 1:10,000 dilution of SYBR Green I stain (Sigma) and were examined using a Nikon Eclipse E800 microscope. Each nucleus was evaluated and assigned a number (0–4) based on the percentage of DNA in each comet tail. One hundred to one hundred fifty nuclei were scored per slide.

ACKNOWLEDGMENTS. Imaging was performed at the Indiana University Light Microscopy Imaging Center. Research was supported by the National Institutes of Health Grants GM075060 (to S.D.M.) and GM60398 (to S.E.J.). S.E.J. is an investigator of the Howard Hughes Medical Institute.

- Margueron R, Reinberg D (2011) The Polycomb complex PRC2 and its mark in life. *Nature* 469(7330):343–349.
- Gan ES, Xu Y, Ito T (2015) Dynamics of H3K27me3 methylation and demethylation in plant development. *Plant Signal Behav* 10(9):e1027851.
- Jacob Y, Michaels SD (2009) H3K27me1 is E(z) in animals, but not in plants. *Epigenetics* 4(6):366–369.
- Charron JB, He H, Elling AA, Deng XW (2009) Dynamic landscapes of four histone modifications during deetiolation in *Arabidopsis*. *Plant Cell* 21(12):3732–3748.
- Lafos M, et al. (2011) Dynamic regulation of H3K27 trimethylation during *Arabidopsis* differentiation. *PLoS Genet* 7(4):e1002040.
- Lu F, Cui X, Zhang S, Jenuwein T, Cao X (2011) *Arabidopsis* REF6 is a histone H3 lysine 27 demethylase. *Nat Genet* 43(7):715–719.
- Oh S, Park S, van Nocker S (2008) Genic and global functions for Paf1C in chromatin modification and gene expression in *Arabidopsis*. *PLoS Genet* 4(8):e1000077.
- Turck F, et al. (2007) *Arabidopsis* TFL2/LHP1 specifically associates with genes marked by trimethylation of histone H3 lysine 27. *PLoS Genet* 3(6):e86.
- Zhang X, et al. (2007) Whole-genome analysis of histone H3 lysine 27 trimethylation in *Arabidopsis*. *PLoS Biol* 5(5):e129.
- Lindroth AM, et al. (2004) Dual histone H3 methylation marks at lysines 9 and 27 required for interaction with CHROMOMETHYLASE3. *EMBO J* 23(21):4286–4296.
- Jacob Y, et al. (2009) ATXR5 and ATXR6 are H3K27 monomethyltransferases required for chromatin structure and gene silencing. *Nat Struct Mol Biol* 16(7):763–768.
- Jacob Y, et al. (2010) Regulation of heterochromatic DNA replication by histone H3 lysine 27 methyltransferases. *Nature* 466(7309):987–991.
- Stroud H, et al. (2012) DNA methyltransferases are required to induce heterochromatic re-replication in *Arabidopsis*. *PLoS Genet* 8(7):e1002808.
- Jacob Y, et al. (2014) Selective methylation of histone H3 variant H3.1 regulates heterochromatin replication. *Science* 343(6176):1249–1253.
- Maluszynska J, Heslop-Harrison JS (1991) Localization of tandemly repeated DNA sequences in *Arabidopsis thaliana*. *Plant J* 1:159–166.
- Cokus SJ, et al. (2008) Shotgun bisulphite sequencing of the *Arabidopsis* genome reveals DNA methylation patterning. *Nature* 452(7184):215–219.

17. Johnson L, Cao X, Jacobsen S (2002) Interplay between two epigenetic marks. DNA methylation and histone H3 lysine 9 methylation. *Curr Biol* 12(16):1360–1367.
18. Soppe WJ, et al. (2002) DNA methylation controls histone H3 lysine 9 methylation and heterochromatin assembly in *Arabidopsis*. *EMBO J* 21(23):6549–6559.
19. Johnson LM, Law JA, Khattar A, Henderson IR, Jacobsen SE (2008) SRA-domain proteins required for DRM2-mediated de novo DNA methylation. *PLoS Genet* 4(11):e1000280.
20. Gilbert DM (2002) Replication timing and transcriptional control: Beyond cause and effect. *Curr Opin Cell Biol* 14(3):377–383.
21. Lee TJ, et al. (2010) *Arabidopsis thaliana* chromosome 4 replicates in two phases that correlate with chromatin state. *PLoS Genet* 6(6):e1000982.
22. Schübeler D, et al. (2002) Genome-wide DNA replication profile for *Drosophila melanogaster*: A link between transcription and replication timing. *Nat Genet* 32(3):438–442.
23. Woodfine K, et al. (2004) Replication timing of the human genome. *Hum Mol Genet* 13(2):191–202.
24. Archambault V, Ikui AE, Drapkin BJ, Cross FR (2005) Disruption of mechanisms that prevent rereplication triggers a DNA damage response. *Mol Cell Biol* 25(15):6707–6721.
25. Arias EE, Walter JC (2007) Strength in numbers: Preventing rereplication via multiple mechanisms in eukaryotic cells. *Genes Dev* 21(5):497–518.
26. Dutta A (2007) Chaotic license for genetic instability and cancer. *Nat Genet* 39(1):10–11.
27. Green BM, Li JJ (2005) Loss of rereplication control in *Saccharomyces cerevisiae* results in extensive DNA damage. *Mol Biol Cell* 16(1):421–432.
28. Zhu W, Dutta A (2006) An ATR- and BRCA1-mediated Fanconi anemia pathway is required for activating the G2/M checkpoint and DNA damage repair upon re-replication. *Mol Cell Biol* 26(12):4601–4611.
29. Bonner WM, et al. (2008) GammaH2AX and cancer. *Nat Rev Cancer* 8(12):957–967.
30. Rogakou EP, Pilch DR, Orr AH, Ivanova VS, Bonner WM (1998) DNA double-stranded breaks induce histone H2AX phosphorylation on serine 139. *J Biol Chem* 273(10):5858–5868.
31. Odell JT, Nagy F, Chua NH (1985) Identification of DNA sequences required for activity of the cauliflower mosaic virus 35S promoter. *Nature* 313(6005):810–812.
32. Iacovoni JS, et al. (2010) High-resolution profiling of gammaH2AX around DNA double strand breaks in the mammalian genome. *EMBO J* 29(8):1446–1457.
33. Seo J, et al. (2014) Genome-wide reorganization of histone H2AX toward particular fragile sites on cell activation. *Nucleic Acids Res* 42(2):1016–1025.
34. Shinohara A, et al. (1993) Cloning of human, mouse and fission yeast recombination genes homologous to RAD51 and recA. *Nat Genet* 4(3):239–243.
35. Cann KL, Dellaire G (2011) Heterochromatin and the DNA damage response: The need to relax. *Biochem Cell Biol* 89(1):45–60.
36. Chiolo I, et al. (2011) Double-strand breaks in heterochromatin move outside of a dynamic HP1a domain to complete recombinational repair. *Cell* 144(5):732–744.
37. Culligan K, Tissier A, Britt A (2004) ATR regulates a G2-phase cell-cycle checkpoint in *Arabidopsis thaliana*. *Plant Cell* 16(5):1091–1104.
38. Curtis MD, Grossniklaus U (2003) A gateway cloning vector set for high-throughput functional analysis of genes in plants. *Plant Physiol* 133(2):462–469.
39. Clough SJ, Bent AF (1998) Floral dip: A simplified method for *Agrobacterium*-mediated transformation of *Arabidopsis thaliana*. *Plant J* 16(6):735–743.
40. Kaufmann K, et al. (2010) Chromatin immunoprecipitation (ChIP) of plant transcription factors followed by sequencing (ChIP-SEQ) or hybridization to whole genome arrays (ChIP-CHIP). *Nat Protoc* 5(3):457–472.
41. Law JA, et al. (2013) Polymerase IV occupancy at RNA-directed DNA methylation sites requires SHH1. *Nature* 498(7454):385–389.
42. Salic A, Mitchison TJ (2008) A chemical method for fast and sensitive detection of DNA synthesis in vivo. *Proc Natl Acad Sci USA* 105(7):2415–2420.
43. Wang C, Liu Z (2006) *Arabidopsis* ribonucleotide reductases are critical for cell cycle progression, DNA damage repair, and plant development. *Plant Cell* 18(2):350–365.

Supporting Information

Feng et al. 10.1073/pnas.1619774114

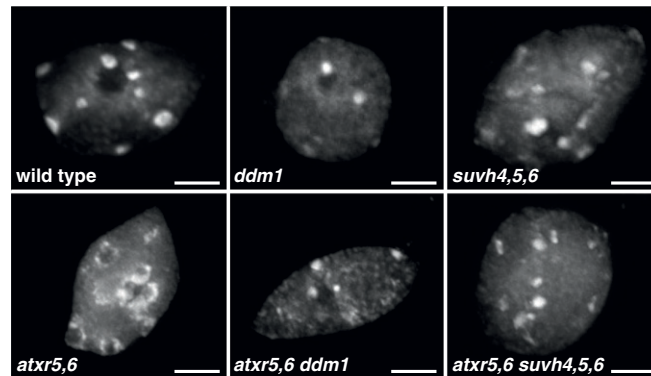


Fig. S1. RACs are correlated with overreplication, not with loss of gene silencing. (Upper Row) *ddm1* and *suvh4,5,6* mutations cause loss of gene silencing but not overreplication. These mutants do not contain RACs. (Lower Row) RAC formation is suppressed in *atxr5,6 ddm1* and *atxr5,6 suvh4,5,6* mutants. (Scale bars: 5 μm .)

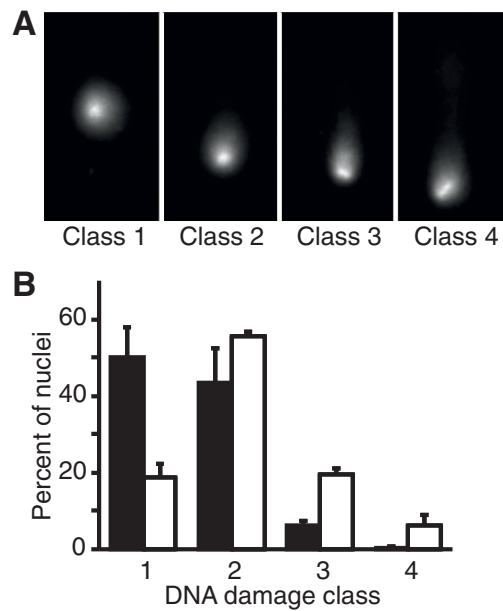


Fig. S2. Detection of DNA damage in comet assays. (A) Classes of nuclei with increasing numbers of double-strand breaks. (B) Quantification of comet assays for wild-type nuclei (black bars) and *atxr5,6* mutants (white bars).

